Prey Size Spectra and Predator:Prey ratios of 7 Species of New Zealand Salps

Authors: Christian K. Fender[1,*], Moira Décima[2], Andres Gutierrez-Rodriguez[3,4], Karen E. Selph[5], Natalia Yingling[1], Michael R. Stukel[1,6]

[1]Department of Earth, Ocean & Atmospheric Science, Florida State University, Tallahassee, FL, USA

[2]Integrative Oceanography Division, Scripps Institution of Oceanography, La Jolla, CA, USA

[3] Sorbonne Université, Station Biologique de Roscoff, Roscoff, France

[4] National Institute of Water and Atmospheric Research, Wellington, New Zealand

[5] Department of Oceanography, University of Hawaii, Honolulu, Hawaii

[6]Center for Ocean-Atmospheric Prediction Studies, Florida State University, Tallahassee, FL, USA

* Correspondance to: Christian K. Fender (ckf18b@my.fsu.edu)

Prepared for submission to the Journal of Marine Biology

Abstract

While the importance of salp grazing has become increasingly apparent in shaping their local ecosystems, little is known about the size ranges of their prey in the field. This study investigated the feeding habits of 7 different species of salp of both solitary and aggregate life stages representing a variety of sizes across subtropical and subantarctic waters east of New Zealand. Scanning electron microscopy was used to examine the gut contents of 58 salps, which were then compared to water column communities sampled via epifluorescence microscopy, FlowCam, and flow cytometry. While most of the gut size spectra and taxonomy resembled ambient waters, substantial differences were found amongst some co-occurring species, such as increased retention of submicron bacteria by *Thalia democratica*. We find that even for such salps capable of feeding on bacteria efficiently, the majority of gut biomass was still made up by nanoplankton and small microplankton. Larger particles were much rarer in the guts than in the water column, potentially suggesting an upper size-threshold in addition to the lower size-threshold that has been the focus of much previous work. Salp carbon-weighted predator to prey size ratios were variable, with the majority falling between 1000:1 and 10000:1 depending largely on the size of the salp. Taken together our results indicate that despite being able to feed on submicron particles, picoplankton are relatively unimportant to the energetics of most salps in this region compared to nanoplankton such as small dinoflagellates and diatoms.

1. Introduction

Salps are a group of large (~1 – 30-cm as adults), suspension-feeding gelatinous zooplankton that filter water through a fine mucous mesh at rates of more than 1000 times the organism's biovolume h^{-1} (Madin et al. 2006). With population doubling times as fast as 8 hours (Aldredge and Madin 1982; Deibel and Lowen 2012), salps are able to form swarms of up to 1000 individuals m^{-3} covering up to 9065 square kilometers in response to favorable conditions (Anderson 1998; Berner 1967). Salps can have clearance rates >100,000 mL ind^{-1} day^{-1} (Madin and Kremer 1995; Perissinnotto and Pakhamov 1998; Sutherland et al. 2010), equivalent to the clearance rate of 450 copepods (Harbison and Gilmer 1976), allowing these blooms to clear water columns of prey so quickly that they can prematurely end spring diatom blooms before surface nutrients were depleted (Bathmann 1988). Despite a growing appreciation for the impact salps may have on ecosystem structure and biogeochemical cycles, relatively little is known of the details regarding their feeding behavior. Only a handful of studies have quantitatively investigated the size of their prey in the field (Madin 1974; Madin and Purcell 1992; Vargas and Madin 2004). The ratio of a predator's size to that of its prey has long been linked to the total length of an ecosystem's food web, where large predator:prey size ratios (hereafter PPSR) result in fewer trophic levels and more efficient transport of primary production to large taxa rather than remineralization (Lindeman 1942; Sheldon et al. 1977; Sherr and Sherr 1988). While it is less frequently recognized, the range of prey sizes a predator can feed on has similar impacts on ecosystem structure. More generalist predators display higher standard deviations in prey size (hereafter SD_{PPSR}) resulting in ecosystems with lower connectance, smaller phytoplankton, and less diversity in phytoplankton size classes (Fuchs and Franks 2011). In short, the PPSR and SD_{PPSR} of the dominant predators in an ecosystem play a strong role in determining its trophic structure.

In other filter-feeding plankton, it is common to observe anywhere from a 5:1 to 100:1 ratio between an organism's size and that of its prey (Hansen et al. 1994; Conley et al. 2018). Pelagic tunicates such as salps, however, exhibit highly dynamic PPSRs as high as 10000:1. They can feed directly on micron-sized picoplankton, but also consume ~1-mm organisms including copepod nauplii, radiolarians, and foraminifera (Madin 1974). Consequently, salps have the potential to simultaneously act as competitors to and predators of a wide variety of protists (Stukel et al. 2021), the group responsible for the majority of phytoplankton grazing in

the pelagic (Calbet and Landry, 2004). Furthermore, as they themselves are part of the diet of at least 202 marine species (Henschke et al. 2016), salps may not act as a net sink as classically believed but instead increase trophic efficiency as previously mentioned. Their presence could thus support economically important species like mackerel (Nishimura 1958), bluefin tuna (Cardona et al. 2012), and anchovies (Mianzan et al. 2001). However, the physiological ability to feed at a 10000:1 ratio does not necessarily mean that this is the range over which most salps feed. As non-selective filter feeders, it is likely this value is largely dependent on the phytoplankton community present. Differing retention efficiencies for small particles have also been reported for a variety of salp species based on removal studies in deck-board incubators (Kremer and Madin 1992; Vargas and Madin 2004), though these techniques often struggle to accurately resolve very small or very large prey. The size of the salp itself likely plays some role as well as there is evidence that small salps may retain smaller particles more efficiently than larger individuals even of the same species (Harbison and McAlister 1979; Kremer and Madin 1992; Stukel et al. 2021). Whether feeding differs intrinsically between species or life stages or if it is purely a function of size is also unknown.

Although traditional microscopic analyses of salp stomach contents have long supported their non-selective nature (Silver 1975; Vargas and Madin 2004; Tanimura et al. 2008), these methods are limited in terms of image resolution such that only large, hard-bodied plankton can be easily identified. A handful of studies have also attempted to directly assess salp gut contents via scanning electron microscopy (SEM), which can resolve particles from the submicron to millimeter size range. Unfortunately, preparatory methods vary, and the focus has similarly always previously been on larger, more easily identifiable prey items like diatoms and thecate dinoflagellates (Madin and Purcell 1992; von Harbou et al. 2011; Ahmad-Ishak 2017). This, along with observations of the mesh spacing in their mucous filters, have led to the commonly accepted view that most salps predominantly feed on particles >1-2 µm in diameter due to the inefficiency with which smaller particles are retained (Harbison and McAlister 1979; Kremer and Madin 1992; Madin and Purcell 1992). Some studies leveraging numerical simulations as well as removal experiments using beads of known size have recently challenged this, suggesting that direct interception of submicrometer particles by the mucous fibers may be a more important source of nutrition than originally believed (Sutherland et al. 2010). Even if retained less efficiently than larger particles, submicron phytoplankton like cyanobacteria are present at far

higher concentrations than larger taxa such that feeding on them may still satisfy a large portion of a salp's carbon quota (Sutherland et al. 2010; Dadon-Pilosof et al. 2019).

In this study, we sought to compare the size composition of prey items in salp stomachs to that of the ambient environment, determine if the resulting size spectra is a function of salp species, size class, or life stage, and see how these demographics impact the PPSR and SD_{PPSR} of salps in a given region. This was accomplished as part of the 2018 Salp Particle Export and Ocean Production (SalpPOOP) study over the Chatham Rise in New Zealand which was designed to investigate how salps affect the ecology and biogeochemistry of the region (Décima et al., in review). The Chatham Rise is notable for its pronounced frontal interactions between northern subtropically influenced waters and the colder, nitrate-rich southern subantarctic influenced waters. This creates a mixing environment where two physico-chemically unique water masses converge, supporting high phytoplankton productivity and biomass for communities usually dominated by picoplankton (Furuya et al. 1986; Pinkerton 2013), which has been previously observed to support large summertime salp blooms. We utilized gut content SEM analysis of 58 individuals composing both life stages of 7 different species over a range of sizes (to our knowledge the most diverse collection of salp diets sampled in a single study) to quantify their diets and compare them to water column plankton populations characterized by flow cytometry, epifluorescence microscopy, and FlowCam imaging.

2. Materials and Methods

2.1 Field Collection

Samples were collected at the Chatham Rise during October 21 - November 21 on the SalpPOOP Cruise (Décima et al., in review). The cruise consisted of 5 quasi-Lagrangian experimental cycles lasting 4-8 days each (Figure 1). Cycle locations were chosen based on net trawls through regions with high potential for salp presence according to previous observations (Nodder et al. 2016). Results for this study come from Cycles 1-4 as salps were not present on Cycle 5. At the beginning of each cycle we deployed of a surface-tethered drifting array to track the chosen water parcel (Landry et al. 2009). Daily dawn and noon deployments of a CTD-Niskin rosette were made to collect water used in live experiments as well as water column profiling. Twice per cycle MOCNESS deployments were made to characterize zooplankton

vertical structure, as well as twice daily oblique Bongo tows down to 200 meters at noon and midnight to determine salp biomass and demographic structure. Ring net surface tows with a 30 liter non-filtering cod-end were also conducted daily for additional salps/zooplankton to be used in live experiments. Once onboard, salps were identified to the species level, sorted by life stage (solitary oozooid or aggregate blastozooid), measured, and sexed (Lükow et al. 2020). Representative samples of each species of salp the first time it was encountered were preserved in 5% formalin < 30 minutes after collections. While this does mean there was potential for digestion between the time the salp was caught and when preservation occurred, processing time was always substantially less than the estimated gut pigment turnover time of 2.8 hours for even the smallest salp caught (Décima et al., in review). Whenever possible these preserved samples included a distribution of size classes, both solitary and aggregate life stages, and were collected in triplicate.

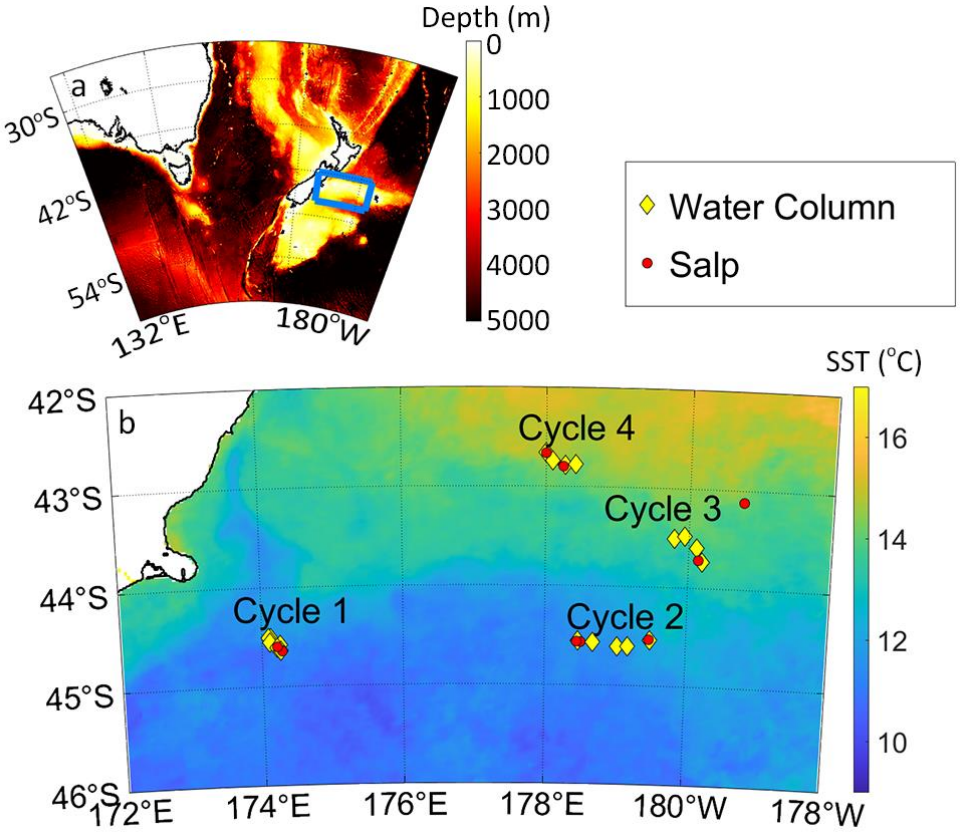

Figure 1. a) TAN1810 cruise study area (blue square) with color denoting depth. b) Magnification of study region with color denoting sea surface temperature. Yellow diamonds

represent CTD deployments to determine water column properties and red circles represent the locations of salp collections for SEM via Bongo or ring net tow.

To characterize the prey community we analyzed 3 types of samples collected daily from Niskin bottles: 250 mL from the base of the mixed layer and the deep chlorophyll max (DCM) were concentrated to 10 mL, with 2 mL imaged using a FlowCam's 10x objective lens to quantify the larger (>3 µm) phytoplankton (Sieracki et al. 1998); an Accuri C6 Plus flow cytometer was used at sea to determine the abundance of *Synechococcus* and eukaryotes collected at 6 depths spanning the euphotic zone with cell size estimated using the front scatter of polystyrene beads of known size (Stukel et al. 2021); additional preserved samples were also collected from the same casts to be run on a Beckman Coulter CytoFLEX S flow cytometer targeting heterotrophic bacteria and *Prochlorococcus* (Selph 2021); preserved and stained epifluorescence microscopy samples were collected and later analyzed on an epifluorescence microscope where cell biomass and abundance were calculated using ImageJ (Taylor et al. 2015).

2.2 Scanning Electron Microscopy

In total, 58 salps representing the species *Salpa thompsoni*, *Pegea confoederata*, *Thalia democratica*, *Soestia zonaria*, *Thetys vagina*, *Salpa fusiformis*, and *Ihlea magalhanica* including both blastozooid and oozooid stages of the first four and a distribution of sizes for the first two were collected. Once ashore, the guts of each organism were excised under a HEPA-filter equipped laminar flow exhaust hood using acid cleaned plastic dissection equipment to minimize contamination. Guts were then placed in either 15 or 50 mL plastic Falcon tubes with a small volume of brine, lacerated, and then vortex mixed for two minutes to release gut contents into solution while minimizing damage to the more fragile phytoplankton. An aliquot of this solution was then filtered onto a 0.2 µm Nuclepore filter, followed by rinses of decreasing salinity in 5 ppt increments for a minimum of 5 minutes each with the final MilliQ water rinse performed twice. This was immediately followed by a dehydration series of increasing ratios of EtOH:MillQ to purge water from the sample, with the final 100% anhydrous EtOH step again performed twice. Finally, a substitution series of increasing ratios of the chemical drying agent HMDS:anhydrous EtOH was conducted with each step lasting a minimum of 10 minutes, with

the final HMDS step being allowed to air dry. Each step was conducted under either a light vacuum or gravity filtration depending on material concentration to minimize loss between treatments. Similar procedures have proven successful in the preparation of both delicate dinoflagellates (Botes et al. 2002; Jung et al. 2009) and bacteria (Koon et al. 2019). The dried filter was then affixed to an Al SEM stub using carbon conductive adhesive tabs and further grounded with a thin piece of carbon conductive tape touching the edge of the filter and the bottom of the stub. Samples were then sputter coated with 10 nm iridium and visualized using an FEI Nova 400 NanoSEM set to an accelerating voltage of 10 kV. 20 random regions of each filter were imaged at 3 different magnifications: ~500x, ~2500x, and ~12000x to target microplankton, nanoplankton, and picoplankton respectively. Since sufficient structural detail could not be observed to definitively identify very small particles, spherical particles within the size range of ~0.4-1.5 um and resembling control images from lab-raised stock cultures of *Prochlorococcus sp.* and *Synechococcus sp.* are instead referred to as bacteria-like particles (BLPs).

2.3 Image Processing

Particles in images were manually outlined using ImageJ (v. 1.52a or 1.53c) to extract the maximum feret length (L), minimum feret length, and area (A). These measurements were used to estimate equivalent spherical diameter (ESD), biovolume (BV), and carbon biomass (BM) assuming a prolate spheroid. To avoid overestimating the size of irregularly shaped particles, we calculated width (W) for a prolate spheroid of measured A and L such that:

$$1) \qquad W = \frac{4\pi}{3} * \frac{A}{L}$$

$$2) \qquad ESD = \sqrt[3]{L * W^2}$$

$$3) \qquad BV = \frac{4\pi}{3} * \frac{L}{2} * \left(\frac{W}{2}\right)^2$$

BM for BLPs was calculated by using flow cytometry to estimate the ratio of *Prochlorococcus*, *Synechococcus*, and heterotrophic bacteria for a given cycle and using that ratio to inform a weighted mean bacterial carbon content for using published allometric relationships (Garrison et al. 2000). The BM of ciliates was estimated as 0.19 pg C μm^{-3} (Putt

and Stoecker 1989) while radiolarians were 0.001 pg C um^{-3} (Stukel et al. 2018). Diatoms and other protists were estimated based on their BV using allometric relationships from Mendendeur and Lessard (2000). White spheres and any unidentified particles were treated as protists for carbon content calculations.

FlowCam image analyses were conducted using FlowCam's dedicated classification software VisualSpreadsheet (v. 4.18.5). First, duplicate images resulting from parabolic flow within the flow cell were manually removed. The particles within the remaining images were then classified based on the quality with which VisualSpreadsheet detected their outlines. For particles where the outline appeared to provide good estimates of L and W, size was calculated for a prolate spheroid as above using Equations 1-3 with the exception that W was left as the directly measured minimum feret length. While this is likely less accurate than utilizing particle area as was done for the SEM images, we frequently noted that particle outlines possessed large holes not representative of overall shape such that area was severely underestimated. For particles where the quality of automatic outline detection was poor, alternative methods used to determine size can be found in the Supplementary Materials. BM was calculated as described above for the salp gut contents.

2.4 Size Spectra and Feeding Distribution Parameter Calculations

For each cycle, the prey items were separated into size bins and their abundance was averaged for each salp species. This abundance was then divided by the size bin width to calculate normalized abundance size spectra (NASS). NASS were similarly produced for each of the methods used to assay the prey field (FlowCam, flow cytometry, and epifluorescence microscopy samples) at each depth and vertically integrated over the euphotic zone. We also present a single composite spectrum representing the geometric mean of each method over the size range where it was relevant. Carbon biomass estimates for both salp and water column measurements were then used in the same way to compute normalized biomass size spectra (NBSS). 95% confidence intervals were calculated using Monte Carlo random resampling. Predator:prey size ratios were calculated using the prey size at which 50% of the total biomass in a salp gut was achieved. Similarly, the standard deviation was calculated as the difference of the mean log prey size at which 84.1% and 15.9% of biomass was achieved divided by 2. The results

are feeding distribution values that are representative of the particles being assimilated by the salp rather than those that are simply ingested.

3. Results

3.1 Salp vs. Ambient Phytoplankton Community Comparisons

Cycle 1 (the cycle closest to the coast) was the only cycle for which any of the three methods used detected particles larger than 120 µm (Figure 2). FlowCam images from Cycle 1 were characterized by a variety of phytoplankton species with a predominance of large centric and pennate diatoms. Many dinoflagellates were also observed. Cycles 3, 4 and 5 were farther from the coast and seemed to support less diatoms with those present of primarily centric morphologies. These cycles displayed an even greater proportion of dinoflagellates, particularly smaller species. Cycle 2 had similarities to both these groups with a moderate number of large pennate diatoms, possibly advected from the coast, but nearly all other particles being small centric diatoms or dinoflagellates. Flow cytometry showed that *Synechococcus*, picoeukaryotes, and heterotrophic bacteria were present in all 5 cycles, but *Prochlorococcus* sp. was only observed in large numbers during Cycles 2 and 5.

Microplankton within salp guts were broadly representative of the taxa present in the water column. When considering the contribution of various size classes to the gut content in each salp gut, picoplankton (<2 µm) generally made up .63-27.12% of total biomass (Figure 1) with a mean of 5.28%, which is substantially lower than the mean contribution in the water column of 17.66%. By far the most abundant objects observed in the guts of all salps regardless of size or species were unidentifiable, smooth, spherical particles (hereafter referred to as “white spheres”) lacking any other notable morphological features and generally of ~3-7 um in diameter but ranging from 0.6-26 µm (Supplementary Figure 1H). Given the broad range in size, it is likely that this category comprises several unrelated groups that had been partially digested, potentially including prymnesiophytes, diatom cysts, dinoflagellate cysts, and/or other nanoflagellates. This, along with large numbers of similarly sized dinoflagellates, likely explains the higher contribution of nanoplankton (2-20 µm) within the gut contents, making up between 19.91% and 99.11% of total biomass with a mean of 76.36%. This is significantly higher than what was observed in the water column as nanoplankton made up only 33.64% of the biomass on

average. Similarly, microzooplankton (20-200 µm) were generally much rarer in the salp guts, making up 0%-78.22% and 18.36% of total biomass on average in contrast with an average of 48.70% in the water column. These discrepancies in the contribution of nanoplankton and microplankton are further considered in the Discussion.

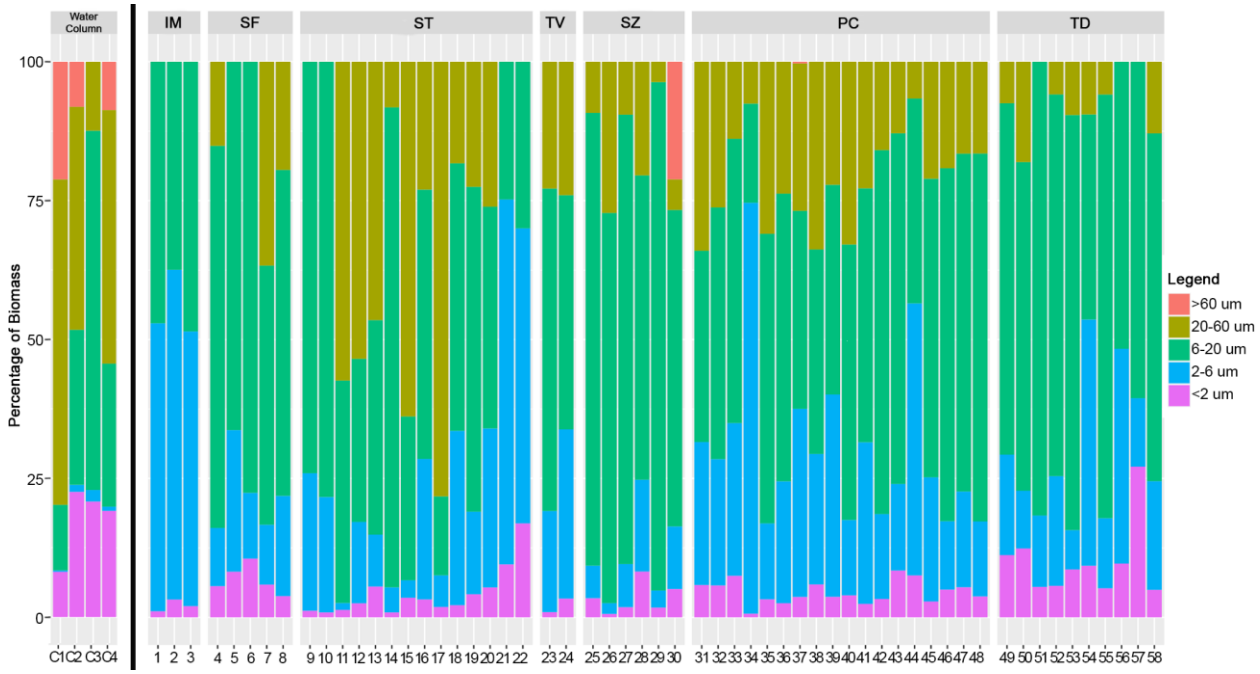

Figure 2. Contribution of particles of various size classes to the total biomass present in the water column of each cycle compared to that of in the guts of each of the 58 salps sampled, with salps grouped by species. See Supplementary Table 1 for more information regarding the numbering of individual salps.

We also compared the average size spectra of prey for each salp species to depth integrated flow cytometry, FlowCam, and epifluorescence microscopy for each of the four cycles from which samples were obtained (Figure 2). Since the volume filtered could not be determined for the salps caught, the units for the normalized abundance size spectra (NASS) and normalized biomass size spectra (NBSS) differ between salp and ambient measurements such that only the shape of the spectra can be compared. This shape represents the relative importance of small vs large particles with steeper (i.e., more negative) spectra indicating more small particles relative to large ones and vice versa. In general, most of the salp spectra match up well to both the water column NASS and NBSS as would be expected for nonselective filter feeders. Every salp species

also shows the same sharp decline in the abundance of submicron particles, which supports inefficient capture of particles <1 um. There are, however, several notable departures from the ambient spectra. For *Thalia democratica* of Cycle 3, the NBSS spectra is much flatter than that of the flow cytometry. While this trend is less apparent for *T. democratica* observed in Cycle 4, it could suggest an increased importance of small particles for this species relative to the others. In contrast, the NASS and NBSS spectra for *Ihlea magalhanica* is far more peaked at 2-4 µm compared to ambient, although rather than suggesting difficulty in retaining small particles this is instead due to the far higher number of white spheres relative to any smaller or larger particles observed in their guts. *Salpa thompsoni* and *Soestia zonaria* of Cycle 1 also display a surprising lack of particles larger than 50 µm despite FlowCam and epifluorescence microscopy showing such particles were present in the water. Similarly, the maximum particle size in the guts of *Thetys vagina* from Cycle 1 was only 13.2 µm. Both species from Cycle 3 and all species from Cycle 4 except *Soestia* show a similar trend.

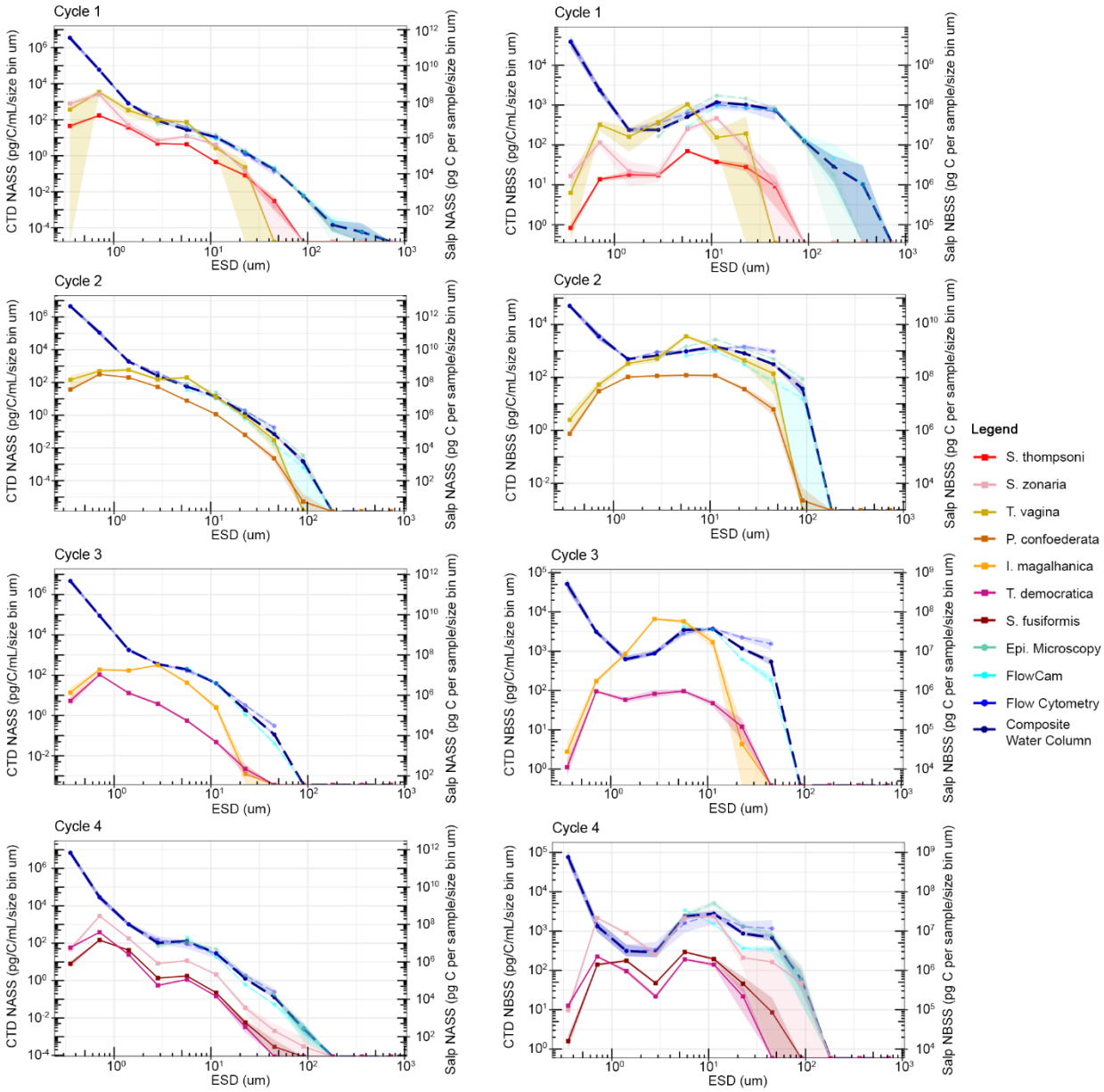

Figure 2. Average Normalized Abundance (left) and Normalized Biomass (right) Size Spectra as a function of prey ESD for Cycles 1-4. Warm colored solid lines denote salp gut contents while cool colored dashed lines represent water column measurements from CTD based devices. The thicker, dark blue line (labeled composite) represents the geometric mean of the ambient measurements. Shaded regions represent 95% confidence intervals for each spectrum. Note the difference in units for y-axes.

3.5 Feeding Distribution Parameters

Most salp species obtained the majority of their carbon from particles less than 15 µm (Figure 3; Supplementary Table 1), likely due to the predominance of small dinoflagellates present in all four cycles coupled with the salps' apparent difficulty in capturing large particles. Notably the smallest species (*Thalia democratica*) which seems better adapted to feeding on small particles, has only a slightly lower average prey size of 8.56 µm. Species from Cycles 1 and 2 (where there were more large particles in the water) such as *Salpa thompsoni* (15.04 µm) and *Soestia zonaria* (12.02 µm) typically fed on slightly larger than average prey. Within species, the size of the salp did not seem to substantially affect the mean prey size. For example, the mean prey size of *Pegea confoederata* was distributed about 11.42 µm for individuals ranging in size by almost an order of magnitude. Even between species no trend with size was observed as the mean prey size of the largest salp *Thetys* is quite comparable at 9.09 µm to that of the smallest species *Thalia*. Likewise, there does not seem to be any trend with salp life stage as the mean prey size was similar for all species for which we encountered both stages: *Soestia zonaria* (blastozooid=11.44 µm; oozoid=12.60 µm), *Pegea confoederata* (blastozooid=11.51 um; oozooid=11.20 µm), *Salpa thompsoni* (blastozooid=15.65 µm; oozooid=12.81 µm), *Thalia democratica* (blastozooid=7.92 µm; oozooid=9.51 µm). *Ihlea magalhanica* had the smallest mean prey size (5.48 µm), because their guts primarily contained small white spheres. The only species for which there was a great deal of variability in mean prey size was *Salpa thompsoni*, which had several individuals where more than 50% of their gut biomass was contained in one or two very large particles, such as polycystine radiolarians, substantially inflating the mean prey size.

Most salp's had predator-prey size ratios (PPSR) between 1000:1 and 10000:1, with only the two largest *S. thompsoni* and the two *T. vagina* feeding at or above 10000:1. Across species, *T. vagina* had the highest PPSR of 17050:1, followed by *P. confoederata* (4199:1), *Salpa fusiformis* (3539:1), *S. zonaria* (3601:1), *I. magalhanica* (3052:1), *S. thompsoni* (2704:1), and *T. democratica* (1475:1). When averaging by life stage as well, oozooids always had a higher PPSR than blastozooids of the same species. There was a clear trend of increasing PPSR with increasing salp size because of the relatively similar prey sizes of all taxa. However, a great deal of variation in PPSR was seen amongst individuals of the same species and size. The PPSRs of smaller *S. thompsoni* range by almost an order of magnitude, while *P. confoederata* and *T.*

democratica possessed many individuals of approximately the same size yet also show PPSRs that vary by a factor of 2-3 in a given size class, reflecting similar variability in mean prey size. Also of note, PPSR was largely independent of which cycle the salp was collected from (and therefore of the phytoplankton community available for it to feed on); 35-40mm *S. fusiformis* and *S. zonaria* collected during Cycle 4, which was much farther from the coast and consequently displayed lower phytoplankton sizes, were comparable to *S. zonaria* and *P. confoederatea* of the same size from the coastal Cycle 1.

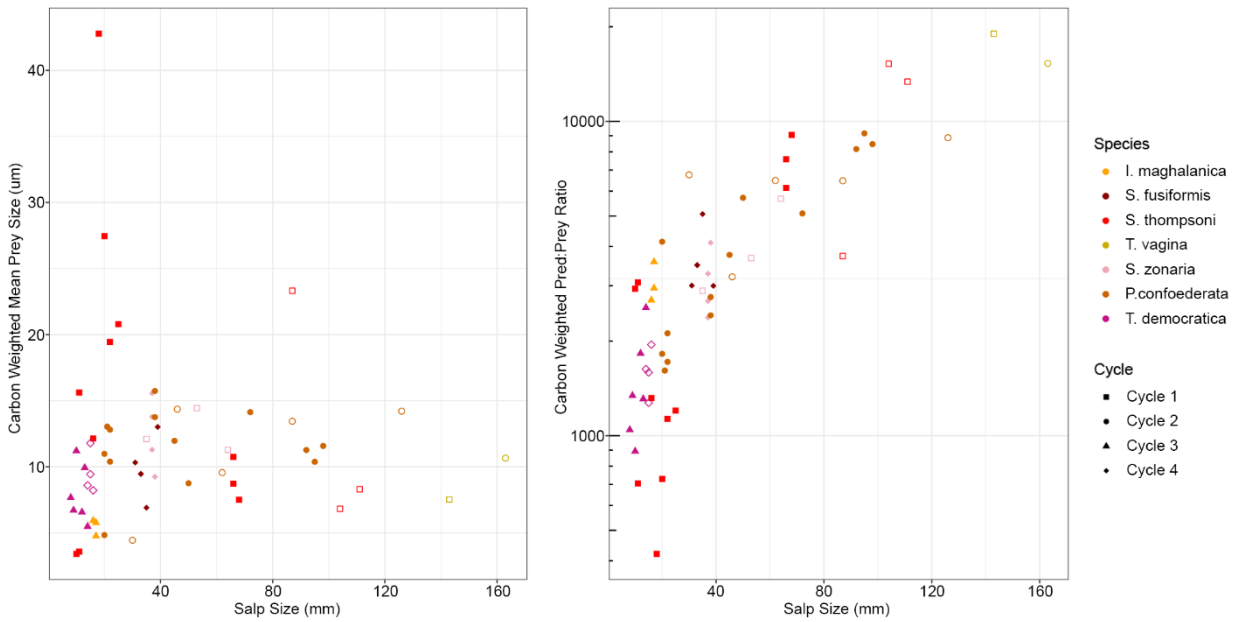

Figure 3. Prey size (left) and predator:prey size ratio (right) at which 50% of gut content biomass is achieved as a function of size for each of the 58 salps collected. Color denotes salp species while shape denotes the cycle in which the sample was collected.

4. Discussion

It has long been accepted that the relationship between predator and prey size has a strong impact on the ecology of an ecosystem (Sheldon et al. 1977, Jennings et al. 2002) and that PPSR broadly varies between zooplankton of different feeding modes (Hansen et al. 1994). For instance, while most zooplankton tend to feed with PPSR's between 10:1 and 100:1 (Hansen et al. 1994, Fuchs & Franks 2010), raptorial protists often feed with PPSR of closer to 3:1 and both pallium-feeding dinoflagellates and some siphonophores can feed at a ~1:1 PPSR (Purcell et al.

1981, Fenchel 1987, Sherr et al. 1991, Naustvoll 2000, Sherr & Sherr 2002). At the other end of the spectrum, pelagic tunicates (salps, doliolids, pyrosomes, and appendicularians) often feed with a predator:prey size ratio >1000:1 (Madin 1974, Crocker et al. 1991, Madin and Purcell 1992, Vargas and Madin 2004, Katechakis et al. 2004). The relative abundance of predators with different PPSR thus has the potential to substantially alter relationships between trophic level and size, with commensurate impacts on energy transfer to larger taxa of commercial importance and carbon export into the deep ocean (Barnes et al. 2010; Michaels & Silver 1988). In addition to a predator's mean PPSR, the range of sizes upon which a predator can feed has the potential to structure food webs. Fuchs and Franks (2010) concluded a dominance of specialized (low SD_{PPSR}) predators that were large relative to their prey (high PPSR) such as copepods would lead to an ecosystem state with lower connectivity between trophic levels, fewer omnivores, more top predators, and greater transfer efficiency to higher trophic levels due to the reduced number of trophic interactions. Conversely, high SD_{PPSR} and/or low PPSR predators like dinoflagellates, raptorial ctenophores, or ciliates led to an ecosystem state with the opposite characteristics.

Here, we carefully quantified not only the mean PPSR for 7 salp species, but also the range of sizes that comprised the majority of their carbon-weighted prey. We found PPSRs that were typically higher (typical values of 1000:1 to 10000:1, with all but 4 individual salps >1000:1 and 70% of our dataset above their maximum reported range of 2236:1, Figure 4) than the summary of estimates for salps reported in a meta-analysis by Fuchs and Franks (2010). These values are also substantially greater than any other taxa in their dataset. As salps are nonselective feeders, a large portion of this difference is probably due to the different prey communities present in the regions from which Fuchs and Franks (2010) acquired their data, which include the Mid-Atlantic Bight (Vargas and Madin 2004), Subarctic Pacific (Madin and Purcell 1992), Florida Current, and Gulf of California (Madin 1974). Their data also include several species not observed in our study such as *Cyclosalpsa affinis*, *Cyclosalpa pinnata*, *Cyclosalpa bakeri*, and *Weelia cylindrica* which are quite distinct physiologically to the species investigated here and may exhibit different feeding characteristics. The individuals in their dataset are also on the small end of our size range, with 3 out of their 5 datasets containing only salps <20 mm and none containing salps > 100 mm (our *T. vagina* were as large as 163 mm). This also likely plays a role in the larger values we observed, because we found little difference

in prey size between large and small salps. Taken together this indicates that the PPSR of salps as a whole may range over two orders of magnitude, which is comparable to the difference between pallium feeding dinoflagellates and suspension feeding copepods. Since the size of salps themselves varies by only around one order of magnitude, this suggests that much of the remaining variability is due to differences in prey communities across sampling locations. Likewise, the range of prey sizes salps feed on can be broader than most other planktonic predators or as narrow as the protists they compete with, again largely varying with the specific conditions of a given study region; the SD_{PPSR} for our study ranged from .1865 to .3405, while Fuchs and Franks (2010) estimated values as high as .5. Attempts to characterize salp predator:prey interactions in models using a single set of generalized parameterizations would fail to capture this regional variability and may lead to significant error when applied to specific ecosystems. Even for global modelling attempts, it seems clear that ascribing a PPSR of 10000:1 is likely an overestimate, and further research is needed to determine an appropriate average for salps as a functional group.

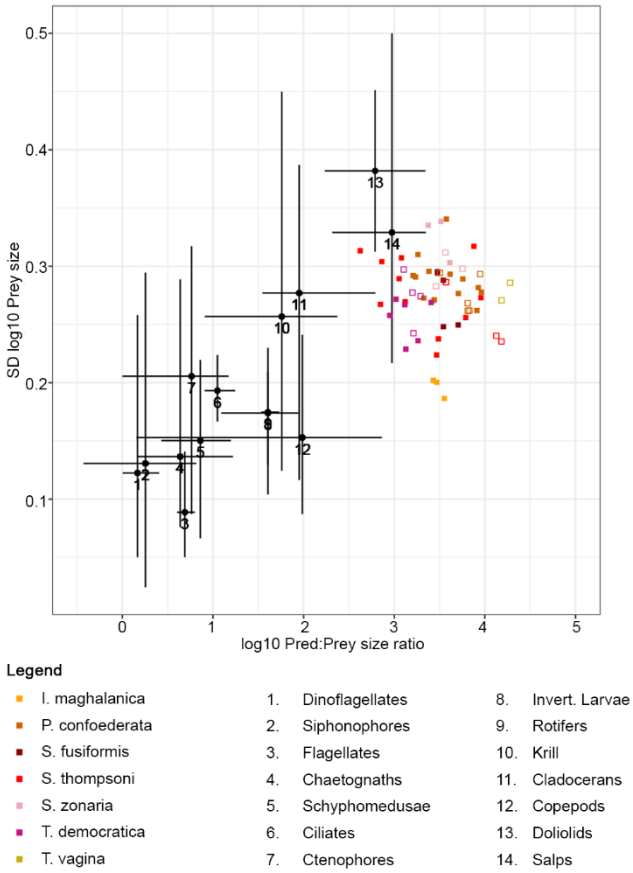

Figure 4. Predator:prey size ratios and standard deviation of prey size for a variety of planktonic predators from Fuchs and Frank (2010; black circles) with bars representing the range. Squares represent individual salp data from this study, with color representing salp species. Filled symbols denote blastozooids and empty symbols denote oozooids. Note that values from this study are carbon weighted.

The low SD_{PPSR} we observed is also probably in part due to the dominance of ~10 µm particles that were ubiquitous across nearly all salps sampled. While many of these were clearly small dinoflagellates or centric diatoms, as mentioned previously the most common particulate items found in salp guts were ~3-7 µm smooth white spheres. These spheres made up 25% of all identified particles and were present even in samples where little to no other recognizable taxa were found. Unknown particles matching this description were also described by both Madin and Purcell (1992) and Ahmad-Ishak et al. (personal communication) and can be seen in the SEM images taken by Caron et al (1989) although they were not discussed. Due to their size and generally spherical shape, we assume that the majority of these particles were nanoplankton for which characteristic features such as flagella had been digested or broken off, although it is likely that this arbitrary categorization includes particles of various origins. For example, some displayed significant silicon signals under electron diffusion spectroscopy and therefore may have been the resting stage cysts of diatoms while others were visually similar to dinoflagellate cysts. Alternatively, some may have been debris or tissue associated with the preparation of the salp itself rather than ingested prey particles. How these particles are treated has a strong impact on how some of our results should be interpreted. For example, the NBSS of *I. magalhanica* showed a strong peak at 2-8 µm due to the exceptionally high numbers of white spheres observed in the guts of all 3 individuals imaged (Figure 2). If these are treated as nanoplankton, as we believe is most likely, our data would suggest feeding on particles of this size class is even more important for this species of salp relative to the others investigated here. If white spheres were not treated as particles and instead excluded from our analysis, the resulting spectra for *I. magalhanica* would be much the same as that of *T. democratica* from the same cycle and would suggest their feeding dynamics are similar. Both salp spectra, however, would then be significantly lacking in particles of this size relative to the ambient spectra. Similar patterns were

observed in the other salp spectra when white spheres were removed, which we interpret as evidence that these particles originated in the water column. We caution that future work, especially if seeking to automate image processing, should take special care with particles in this size class.

The degree to which each salp can efficiently retain picoplanktonic prey is determined by the mesh spacing of their feeding filter, which varies between species (Bone et al 2003). We estimated retention efficiency (hereafter RE) by dividing the NASS of each salp species by that of the water column for each size class (proportional to the clearance rate) and dividing the result by the average clearance rate for the size bins of particles expected to be retained with 100% efficiency (proportional to the filtration rate). Here we chose to average over 8-32 µm as particles with ESDs slightly smaller than this will sometimes possess aspect ratios allowing them to pass through the feeding mesh and our results show that particles larger than this were frequently absent from salp guts. For most salps, we find 100% retention for 1-4 µm particles (Figure 5), but much lower retention for submicron particles, which agrees with many previous studies (Harbison and Gilmer 1976; Kremer and Madin 1982; Caron et al. 1989; Sutherland et al. 2010; Nishikawa and Tsuda 2021; Stukel et al. 2021). With respect to the larger prey size classes, however, by far the most striking result of our calculations is the rapid decline in retention for most salps at particle sizes >16 µm. As mentioned previously, this resulted in a surprisingly low contribution of microplankton to the total salp gut biomass compared to what was found in the water column. Indeed, only a single salp had a substantial portion of its total gut biomass made up by >60 µm particles (Figure 2), and that contribution was made up entirely by a single large dinoflagellate.

Typically, all particles above the width of a salp's mucous feeding mesh are considered to be retained with 100% efficiency. However, previous studies used only a selection of particles of up to ~10 µm in size, so it is unclear whether salp's feed efficiently on these larger particles. Several factors could lead to an underestimate of our RE for these size classes. For example, to avoid biasing our size spectra low or overcounting more fragile species, we chose to exclude all particles in the salp guts which were clearly broken (less than ¾ their assumed true length). This had no impact on BLPs as they were always whole in the guts, negligible impacts on the initial counts of small dinoflagellates and centric diatoms, and only marginally affected our final RE

estimates. It did, however, result in 82% of the initial pennate diatom and >90% of initial large dinoflagellate counts being disqualified. It is possible that larger, fragile organisms like chains of pennate diatoms were separated into solitary cells and/or further fragmented as the salp's filter was passed through the esophagus and into the stomach or even as a result of our preparations in the lab. Indeed, deckboard disappearance experiments, which would not suffer this bias, performed with *S. thompsoni* on our cruise did not show a consistent decrease in RE for particles up to 30-µm ESD (Stukel et al. 2021). However, the incubation experiments of Vargas and Madin (2004) did find substantially lower retention efficiencies of 30-40% for 60-µm diatoms in *Salpa cylindrica* and *Cyclosalpa affinis* in the Mediterranean. They proposed the existence of a size threshold for large particles at which the likelihood of bolus formation and subsequent expulsion of the feeding filter (Harbison and Gilmer 1976; Harbison et al. 1986; Vargas and Madin 2004) further decreases their already low relative abundance in the guts. To this end we noted a complete absence of large, spiny pennate diatoms like *Chaetoceros* sp. (both solitary cells and chains) and *Proboscia* sp. which dominated the larger size classes in the FlowCam. Similar discrepancies were observed by Ahmad-Ishak et al. (2017) who noted that while both former groups made up large biovolumes in their study region according to light microscopy, only *Proboscia alata* was found in the guts of *S. fusiformis* and *T. democratica* via SEM. Our understanding of the conditions under which boluses form are still too poor to allow for more than speculation here. For the time being, however, these uncertainties are reflected in the exceptionally large confidence intervals for our estimates of RE on >8-µm particles which frequently extend to 100% RE. We thus encourage readers to consider the true REs for these particles as within this range rather than the mean values we present.

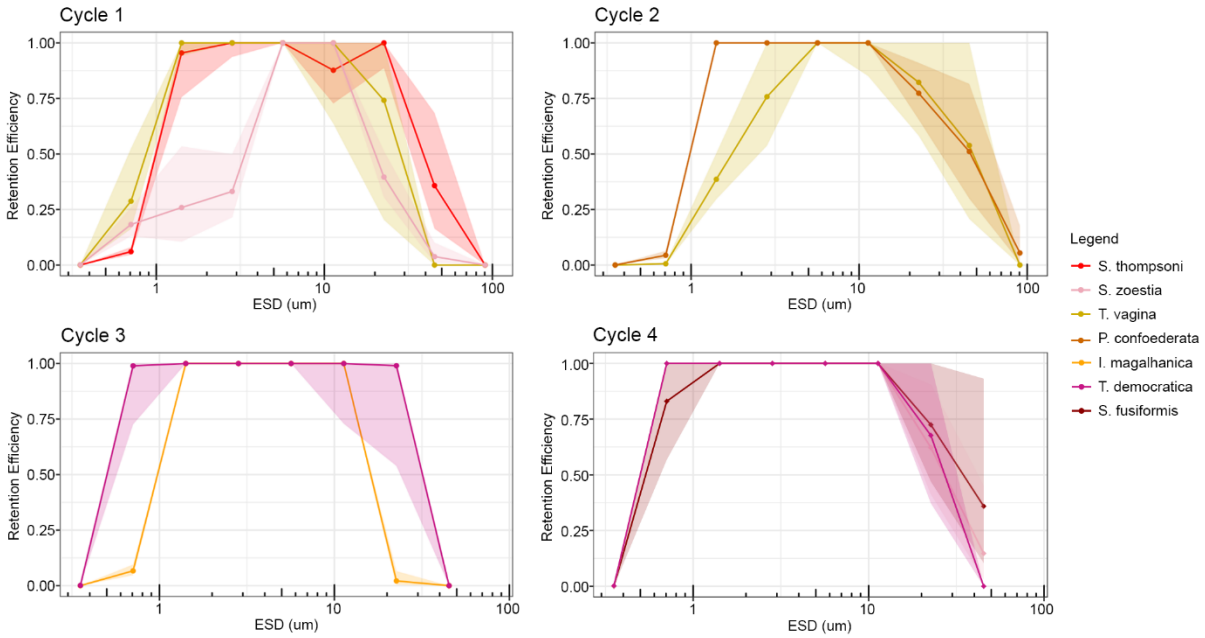

Figure 5. Average retention efficiency for each species of salp found in each cycle, assuming filtration rate is equivalent to the clearance rate on 8-32 um cells. Shaded areas represent 95% confidence intervals.

While only a handful of studies have attempted to quantify the width of the mucous feeding filters in salps (Silver and Bruland 1981; Bone et al. 1991; Bone et al. 2000; Sutherland et al. 2010), the mesh of *T. democratica* has been observed to be quite fine at 0.9 x 0.9 µm (Bone et al. 2003). This is one explanation for their markedly higher retention efficiencies for submicron particles compared to other species (Figure 5). Indeed, several studies have reported *T. democratica* feeding at varying levels of efficiency on bacteria (Mullen 1983; Vargas and Madin 2004). Higher retention of small particles could also be related to the size of the individual as several studies have reported higher retention efficiencies for small particles in smaller salps (Harbison and McCalister 1979; Kremer and Madin, 1992, Stukel et al. 2021) potentially due to isometric scaling of the mesh width to organism size (Sutherland et al 2010). Indeed, *S. fusiformis* REs begin to fall off below 1-2 µm similarly to *S. thompsoni* and *T. vagina* yet they are substantially higher for submicron particles. We postulate that this is due to the significantly lower mean size of *S. fusiformis* (34.7 mm) captured compared to that of our *S. thompsoni* (50.3 mm) and *T. vagina* (153 mm). When also considering *S. thompsoni* of different

size classes, we again find smaller blastozooids display higher REs for submicron particles and larger oozooids show lower REs for particles < 4 µm. These observations match remarkably well to those predicted by the equation for *S. thompsoni* size specific clearance rate given in Stukel et al. (2021), which describes mesh diameter as an allometrically-scaling function of salp size, and a similar trend can also be seen for *P. confoederata* (Figure 6).

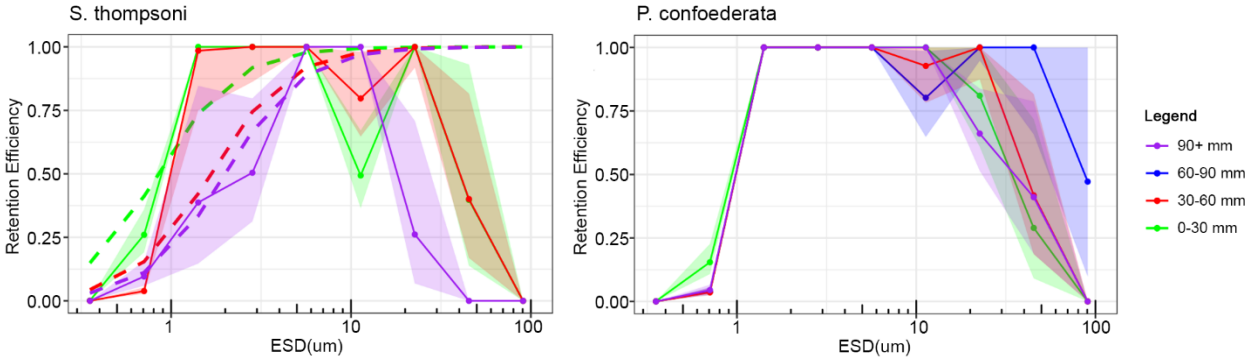

Figure 6. Retention Efficiencies for different sizes of *S. thompsoni* (left) and *P. confoederata* (right) assuming a filtration rate equal to the clearance rate for 8-32 um particles. Solid lines represent REs averaged by salp size class, dashed lines represent REs calculated using the size resolved clearance rate equation from Stukel et al. (2021) for *S. thompsoni*, and shaded intervals represent 95% confidence intervals.

Variation in how differently sized particles are fed on by salps is of great ecological importance as it determines how their feeding structures the plankton community around them, but the contribution of different size classes to the total biomass ingested by the salp is also relevant from the perspective of salp energetics. For example, even if inefficient submicron feeding results in larger numbers of bacteria being removed from the water than traditionally believed as has been proposed (Sutherland et al. 2010; Dadon-Pilosof et al. 2019), the lower total carbon content per cell attributable to small particles compared to that of rarer but more efficiently retained and carbon-rich particles means the former may still be relatively inconsequential to a salp's diet. We find that that is the case here as although large numbers of BLPs were found in the guts, for nearly all salps sampled most of the total gut biomass was made

up by >6 µm particles with generally lower contributions by picoplankton than were present in the water column (Figure 2). Indeed, most showed carbon weighted mean prey sizes of 10-15 µm (Figure 3), which is in agreement with Stukel et al.'s (2021) results for incubated *S. thompsoni* for which >8 µm particles made up most of their diet. Likewise, a variety of reports suggest that small diatoms and dinoflagellates make up the bulk of the diet for many different species of salps (Vargas and Madin 2004; Tanimura et al. 2008; Ahmad-Ishak et al. 2017) sometimes regardless of sampling location or season (von Harbou et al. 2011), implying this ~10 µm size class may represent a sweet spot between numerical abundance in the water column and carbon content. This contrasts with the findings of Sutherland et al. (2010), who reported submicron particles alone could make up more than 100% of the carbon requirement for *P. confoederata*. However, this conclusion hinged on their assumption that only the outer 0.1 µm of ingested cells were digested. When instead assuming complete digestion of all particles, as we do here, they also found the majority of carbon came from 1-10 µm particles such as flagellates and small diatoms. The true degree of digestion will of course vary based on the composition of a given particle and the gut turnover time of the salp in question such that the effective nutritional value of a particle is determined by something between its surface area and its volume (Sutherland et al 2010). Until such time as we can better predict the nutritional values for different plankton types, we believe our results to be close to the true mean prey size of salps in this region.

5. Conclusion

Overall, our results indicate that within the 1-30 µm size range, salp diets for the seven species investigated here largely reflect the size composition of plankton in the surrounding water. Feeding on submicron particles, however, appears to be dependent on both salp species and size. *T. democratica*, perhaps due to its smaller average size, was able to retain even submicron particles efficiently whereas most of the larger species such as *T. vagina*, *S. thompsoni*, and *P. confoederata* showed reduced retention efficiencies below 1 um. Retention for particles >1 µm was high except for a consistent decrease in efficiency for >16 µm particles across all salps which may be the result of difficulty ingesting larger particles or an artefact of our sample preparation. Regardless, salps fed at predator:prey size ratios ranging from 1475:1 for the smallest *T. democratica* to 17050:1 for the largest *T. vagina* with most falling between

1000:1 and 10000:1. This order of magnitude variability is primarily due to the large range of sizes over which salps can occur, which suggests that different parameterizations are likely needed to model the impact of salp feeding across communities with different species and/or size compositions. Future work to investigate prey size spectra across a broader range of salp sizes and species is necessary to disentangle the potentially confounding impacts of these factors. To that end, deckboard disappearance rate experiments using natural prey (Stukel et al. 2021), rather than synthetic beads, analyzed by a variety of methods with overlapping effective size ranges (SEM, flow cytometry, FlowCam or other similar imaging platforms, light microscopy, etc.) and paired with direct gut content analysis should provide the greatest resolution for *in situ* salp feeding size spectra.

7. Acknowledgements

We would like to thank the captain and crew of the R/V Tangaroa for help in the deployment of equipment as well as our many collaborators in the SalpPOOP project including Scott Nodder, Sadie Mills, Florian Lüskow, Morgan Meyers, Sarah Searson, Siobhan O'Connor, Karl Safi, Adriana Lopes dos Santos, and Fenella Deans.

8. Funding

This study was made possible by funding from the Ministry for Business, Innovation and Employment (MBIE) of New Zealand, NIWA Coast and Oceans Food Webs (COES) and Ocean Flows (COOF), and the Royal Society of New Zealand Marsden Fast-track award to M. Decima, and by U.S. National Science Foundation awards OCE- 1756610 and 1756465 to M.R.S. and K.E.S.

9. Conflict of Interests

The authors declared no conflict of interests.

9. Data Availability

All data is accessible on the Biological and Chemical Oceanography Data Management Office website (https://www. bco-dmo.org/project/754878).

7. References

Aldredge AL, Madin LP (1982) Pelagic tunicates: unique herbivores in the marine plankton. Bioscience 32(8): 655-663

Anderson V (1998) Salp and pyrosomid blooms and their importance in biogeochemical cycles. The biology of pelagic tunicates. 125-137

Barnes C, Maxwell D, Reuman DC, Jennings S (2010) Global patterns in predator–prey size relationships reveal size dependency of trophic transfer efficiency. Ecology 91(1): 222-232 DOI: 10.1890/08-2061.1

Bathmann UV (1988) Mass occurrence of Salpa fusiformis in the spring of 1984 off Ireland : implications for sedimentation processes. Mar Biol 97:127-135

Berner LD (1967) Distributional atlas of Thaliacea in the California Current region. Calcofi Atlas No. 8, California Marine Research Committee

Bone Q, Braconnot JC, Ryan KP (1991) On the pharyngeal feeding filter of the salp Pegea confoederata (Tunicata: Thaliacea). Acta Zoologica 72(1):55-60

Bone Q, Carre C, Ryan KP (2000) The endostyle and the feeding filter in salps (Tunicata). Journal of the Marine Biological Association of the United Kingdom 80(3):523-534

Bone Q, Carre C, Chang P (2003) Tunicate feeding filters. Journal of the Marine Biological Association of the United Kingdom 83(5):907-919

Botes L, Price B, Waldron M, Pitcher GC (2002) A simple and rapid scanning electron microscope preparative technique for delicate “Gymnodinioid” dinoflagellates. Microscopy research and technique 59(2):128-130

Calbet A, Landry MR (2004) Phytoplankton growth, microzooplankton grazing, and carbon cycling in marine systems. Limnology and Oceanography 49(1):51-57

Cardona L, Álvarez de Quevedo I, Borrell A, Aguilar A (2012) Massive consumption of gelatinous plankton by Mediterranean apex predators. PloS one 7(3):e31329

Conley KR, Lombard F, Sutherland KR (2018) Mammoth grazers on the ocean's minuteness: a review of selective feeding using mucous meshes. Proceedings of the Royal Society B: Biological Sciences 285(1878)

Crocker KM, Alldredge AL, Steinberg DK (1991) Feeding rates of the doliolid, Dolioletta gegenbauri, on diatoms and bacteria. Journal of plankton research 13(1):77-82

Dadon-Pilosof A, Lombard F, Genin A, Sutherland KR, Yahel G (2019) Prey taxonomy rather than size determines salp diets. Limnology and Oceanography 64(5):1996-2010

Deibel D, Lowen B (2012) A review of the life cycles and life-history adaptations of pelagic tunicates to environmental conditions. ICES Journal of Marine Science 69(3):358-369

Fenchel T (1987) Ecology of Protozoa: The biology of free-living phagotropic protists. Springer-Verlag

Furuya K, Hasumotoa H, Nakai T, Nemoto T (1986) Phytoplankton in the Subtropical Convergence during the austral summer: community structure and growth activity. Deep-Sea Research 33:621-630

Garrison DL, Gowing MM, Hughes MP, Campbell L, Caron DA, Dennett MR, et al (2000) Microbial food web structure in the Arabian Sea: a US JGOFS study. Deep Sea Research Part II: Topical Studies in Oceanography 47(7-8):1387-1422

Hansen B, Bjornsen PK, Hansen PJ (1994) The size ratio between planktonic predators and their prey. Limnology and Oceanography 39(2): 395-403 DOI: 10.4319/lo.1994.39.2.0395.

Harbison GR, Gilmer RW (1976) The feeding rates of the pelagic tunicate Pegea confederata and two other salps 1. Limnology and Oceanography 21(4):517-528

Harbison GR, McAlister VL (1979) The filter-feeding rates and particle retention efficiencies of three species of Cyclosalpa (Tunicata, Thaliacea) 1. Limnology and Oceanography 24(5):875-892

Harbison GR, McAlister VL, Gilmer RW (1986) The response of the salp, Pegea confoederata, to high levels of particulate material: Starvation in the midst of plenty 1. Limnology and Oceanography 31(2):371-382

Henschke N, Everett JD, Richardson AJ, Suthers IM (2016) Rethinking the role of salps in the ocean. Trends in ecology & evolution 31(9):720-733

Ishak NHA, Clementson LA, Eriksen RS, van den Enden RL, Williams GD, Swadling KM (2017) Gut contents and isotopic profiles of Salpa fusiformis and Thalia democratica. Marine Biology 164(6):1-10

Jennings S, Warr KJ, Mackinson S (2002) Use of size-based production and stable isotope analyses to predict trophic transfer efficiencies and predator-prey body mass ratios in food webs. Marine Ecology Progress Series 240:11-20

Jung SW, Joo HM, Park JS, Lee JH (2010) Development of a rapid and effective method for preparing delicate dinoflagellates for scanning electron microscopy. Journal of applied phycology 22(3):313-317

Katechakis A, Stibor H (2004) Feeding selectivities of the marine cladocerans Penilia avirostris, Podon intermedius and Evadne nordmanni. Marine Biology 145(3):529-539

Koon MA, Ali KA, Speaker RM, McGrath JP, Linton EW, Steinhilb ML (2019) Preparation of Prokaryotic and Eukaryotic Organisms Using Chemical Drying for Morphological Analysis in Scanning Electron Microscopy (SEM). Journal of Visualized Experiments 143:e58761

Kremer P, Madin LP (1992) Particle retention efficiency of salps. Journal of Plankton Research 14(7):1009-1015

Landry MR, Ohman MD, Goericke R, Stukel MR, Tsyrklevich K (2009) Lagrangian studies of phytoplankton growth and grazing relationships in a coastal upwelling ecosystem off Southern California. Progress in Oceanography, 83(1-4):208-216

Lindeman RL (1942) The trophic-dynamic aspect of ecology. Ecology, 23(4):399-417

Lüskow F, Pakhomov EA, Stukel MR, Décima M (2020) Biology of Salpa thompsoni at the Chatham Rise, New Zealand: demography, growth, and diel vertical migration. Marine Biology 167(12):1-18

Madin LP (1974) Field observations on the feeding behavior of salps (Tunicata: Thaliacea). Marine Biology 25(2):143-147

Madin, LP (1982) Production, composition and sedimentation of salp fecal pellets in oceanic waters. Marine Biology 67(1):39-45

Madin, LP, Purcell JE (1992) Feeding, metabolism, and growth of Cyclosalpa bakeri in the subarctic Pacific. Limnology and Oceanography 37(6):1236-1251

Madin, LP, Kremer P (1995) Determination of the filter-feeding rates of salps (Tunicata, Thaliacea). ICES Journal of Marine Science 52(3-4):583-595

Madin, LP et al (2006) Periodic swarms of the salp Salpa aspera in the Slope Water off the NE United States: Biovolume, vertical migration, grazing, and vertical flux. Deep Sea Res. Part I 53:804-819

Menden-Deuer S, Lessard EJ (2000) Carbon to volume relationships for dinoflagellates, diatoms, and other protist plankton. Limnology and oceanography 45(3):569-579

Mianzan H et al (2001) Feeding on survival-food: gelatinous plankton as a source of food for anchovies. Hydrobiologia 451:45-53

Michaels AF, Silver MW (1988) Primary production, sinking fluxes and the microbial food web. Deep-Sea Research 35(4):473-490

Naustvoll LJ (2000) Prey size spectra and food preferences in thecate heterotrophic dinoflagellates. Phycologia 39(3):187-198

Nishimura S (1958) Quelques remarques sur I'ingestion du salpe, Salpa fusiformis Curvier, chez les maquereaux peches dans la mer du Japan orientale. Annu. Rep. Jap. Sea Reg. Fis. Res. Lab. 4:105–112

Nodder SD, Chiswell SM, Northcote LC (2016) Annual cycles of deep-ocean biogeochemical export fluxes in subtropical and subantarctic waters, southwest Pacific Ocean. Journal of Geophysical Research: Oceans 121(4):2405-2424

Pinkerton MH (2013) Ecosystem modelling of the Chatham Rise. NIWA Client, 111

Purcell JE (1981) Dietary composition and diel feeding patterns of epipelagic siphonophores. Mar Biol 65:83–90

Putt M, Stoecker DK (1989) An experimentally determined carbon: volume ratio for marine "oligotrichous" ciliates from estuarine and coastal waters. Limnology and Oceanography, 34(6):1097-1103

Selph KE (2021) Enumeration of marine microbial organisms by flow cytometry using near-UV excitation of Hoechst 34580-stained DNA. Limnology and Oceanography: Methods, 19(10):692-701

Sieracki CK, Sieracki ME, Yentsch CS (1998) An imaging-in-flow system for automated analysis of marine microplankton. Marine Ecology Progress Series 168:285-296

Sheldon RW, Sutcliffe Jr WH, Paranjape MA (1977) Structure of pelagic food chain and relationship between plankton and fish production. Journal of the Fisheries Board of Canada 34(12):2344-2353

Sherr E, Sherr B (1988) Role of microbes in pelagic food webs: a revised concept. Limnology and oceanography 33(5):1225-1227

Sherr EB, Sherr BF, McDaniel J (1991) Clearance Rates of Less-Than-6 Mu-M Fluorescently Labeled Algae (Fla) by Estuarine Protozoa - Potential Grazing Impact of Flagellates and Ciliates. Marine Ecology-Progress Series 69(1-2):81-92

Sherr EB, Sherr BF (2002) Significance of predation by protists in aquatic microbial food webs. Antonie Van Leeuwenhoek International Journal of General and Molecular Microbiology 81(1-4):293-308

Silver MW (1975) The habitat of Salpa fusiformis in the California Current as defined by indicator assemblages 1. Limnology and Oceanography 20(2):230-237

Silver MW, Bruland KW (1981) Differential feeding and fecal pellet composition of salps and pteropods, and the possible origin of the deep-sea flora and olive green 'cells'. Marine Biology 62:263-273

Stukel MR, Biard T, Krause J, Ohman MD (2018) Large Phaeodaria in the twilight zone: Their role in the carbon cycle. Limnology and Oceanography 63(6):2579-2594

Stukel MR, Décima M, Selph KE, Gutiérrez-Rodríguez A (2021) Size-specific grazing and competitive interactions between large salps and protistan grazers. Limnology and Oceanography, 66(6):2521-2534

Sutherland KR, Madin LP (2010) A comparison of filtration rates among pelagic tunicates using kinematic measurements. Marine biology 157(4):755-764

Tanimura A, Kawaguchi S, Oka N, Nishikawa J, Toczko S, Takahashi KT et al (2008) Abundance and grazing impacts of krill, salps and copepods along the 140^ oE meridian in the Southern Ocean during summer. Antarctic Science, 20(4):365

Taylor AG, Landry MR, Selph KE, Wokuluk JJ (2015) Temporal and spatial patterns of microbial community biomass and composition in the Southern California Current Ecosystem. Deep Sea Research Part II: Topical Studies in Oceanography 112:117-128

Vargas CA, Madin LP (2004) Zooplankton feeding ecology: clearance and ingestion rates of the salps Thalia democratica, Cyclosalpa affinis and Salpa cylindrica on naturally occurring particles in the Mid-Atlantic Bight. Journal of plankton research 26(7):827-833

von Harbou L, Dubischar CD, Pakhomov EA, Hunt BP, Hagen W, Bathmann UV (2011) Salps in the Lazarev Sea, Southern Ocean: I. Feeding dynamics. Marine Biology 158(9):2009-2026